frontiers | Frontiers in Materials

ORIGINAL RESEARCH
published: 27 June 2022
doi: 10.3389/fmats.2022.893072

Colloidal Stability of Magnetite Nanoparticles Coated by Oleic Acid and 3-(N,N-Dimethylmyristylammonio) propanesulfonate in Solvents

Liu Li[1], *Decai Li*[1,2]* *and Zhili Zhang*[1]

[1]School of Mechanical, Electronic and Control Engineering, Beijing Jiaotong University, Beijing, China, [2]State Key Laboratory of Tribology, Tsinghua University, Beijing, China

In order to understand the factors affecting the colloidal stability in the carrier liquids of different ferrofluids, magnetite nanoparticles coated by surfactants 3-(N,N-dimethylmyristylammonio)propanesulfonate (DP) and oleic acid (OA) were fabricated as dispersions in diverse colloidal systems. The OA-coated magnetite could only be dispersed in the apolar carrier liquid ($\varepsilon_r < 5$), while DP-coated magnetite particles could establish a stable colloidal system in the polar base liquid ($\varepsilon_r > 5$) such as water and ethanol. The colloidal stability of OA-coated particles in the apolar solvents was mainly attributed to the steric repulsion of its outer thick liquid shell (~3 nm). Due to the absence of steric repulsion on the solid thin shell (~1 nm) on DP-coated magnetite, DP-coated particles could not be dispersed in the apolar liquid. In the polar liquid-based ferrofluids, DP-coated magnetite could form an electric double layer (EDL). The total Gibbs interfacial energy was analyzed based on Van Oss-Chaudhry-Good and DLVO theory to describe the behaviors of coated particles in solvents. In the case of neutral (pH = 7) water-based colloidal, DP-coated magnetite could establish an energy barrier of ~2.2 k_BT to prevent the particles from precipitation. Bare magnetite particles could form a relatively fragile colloid in a water system with an energy repulsion of ~1.2 k_BT. In contrast, OA-coated magnetite exhibited a severe phase separation in a water-based colloidal system due to its net attraction ~ −1.3 k_BT.

Keywords: ferrofluids, nanoparticls, surfactants, electrical double layer, DLVO theories

OPEN ACCESS

Edited by:
Wenbo Wang,
Inner Mongolia University, China

Reviewed by:
Andrew Jackson,
Lund University, Sweden
R. P. Pant,
National Physical Laboratory (CSIR), India

***Correspondence:**
Decai Li
lidecai@tsinghua.edu.cn

Specialty section:
This article was submitted to Polymeric and Composite Materials, a section of the journal Frontiers in Materials

Received: *09 March 2022*
Accepted: *05 May 2022*
Published: *27 June 2022*

Citation:
Li L, Li D and Zhang Z (2022) Colloidal Stability of Magnetite Nanoparticles Coated by Oleic Acid and 3-(N,N-Dimethylmyristylammonio) propanesulfonate in Solvents. Front. Mater. 9:893072. doi: 10.3389/fmats.2022.893072

INTRODUCTION

Ferrofluids are stable colloidal suspensions composed of carrier liquids and nanosized magnetic iron oxide particles (Rodríguez-Arco et al., 2011a; Jain et al., 2011; Medeiros et al., 2012; Pathak et al., 2019; Kumar et al., 2020). Due to the standard nanodiameter of iron oxide particles, magnetic colloidal suspension maintains its stability under gravitational and magnetic field gradients. As a combination of magnet and liquid, ferrofluids can be controlled by the magnetic field, which makes it become a promising candidate for many specific applications (Dailey et al., 1999; Hartshorne et al., 2004; Torres-Díaz and Rinaldi, 2014). The magnetic particles in ordinary ferrofluids are generally coated by a variety of long-chain organic surfactants (Hong et al., 2008; Okabe et al., 2017; Shi et al., 2018; Kumar et al., 2021; Kumar et al., 2022). These surfactants have a polar hydrophilic head group and an apolar hydrophobic end (Sawisai et al., 2019). The surfaces of magnetic iron oxide are

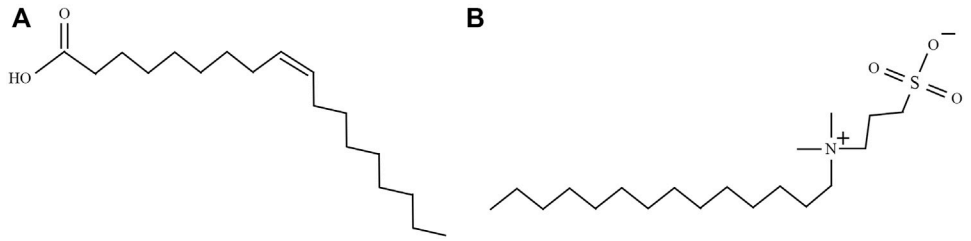

FIGURE 1 | Structural formulae of two kinds of surfactants: **(A)** oleic acid (OA) and **(B)** 3-(N,N-dimethylmyristylammonio)propanesulfonate (DP).

generally hydrophilic, which enables these surfaces to be combined with the polar head group of surfactants. The long chain of surfactants provides nanoparticles with a steric repulsion force which prevents the colloidal system from aggregation (Rodríguez-Arco et al., 2011b).

Oleic acid (OA), as one of the easily obtained classical surfactants, has been extensively studied in recent years (Lobaz et al., 2012; Etemadi and Plieger, 2020; Saputro et al., 2020). The oleic acid has a polar carboxyl group, allowing it to be attached to the surface of nanoparticles (López-López et al., 2005; Zhang et al., 2006; Rodríguez-Arco et al., 2011b; Gyergyek et al., 2011). The other side of oleic acid has a long C_{18} chain, making nanoparticles stable in colloidal solvents. The mechanisms of colloidal stability in ferrofluids with non-polar based liquid have been widely studied (López-López et al., 2005; Gyergyek et al., 2011). The association between stability and interfacial free energy in ferrofluids was proposed by Lopez-Lopez et al. (2005). The calculation of surface free energy of OA-coated magnetic particles is based on formal VOCG theory by calculating Lifshitz-van der Waals forces (LW forces) and acid-base interfacial interactions (AB interactions) (van Oss, 1993). Gyergyek et al. (2011) group take an additional steric repulsion into account, which is interpreted as the influence of the surfactants overlapping between neighbor particles (Gyergyek et al., 2011). However, oleic acid-coated nanoparticles can only be dispersed in the carrier liquid with a dielectric constant ($\varepsilon_r < 5$) (López-López et al., 2005). The explanation of the instability of polar colloidal could be the hydrophobic/hydrophilic bond between particles and carrier base liquid. Oleic acid-covered particles would have a phase separation when they were dispersed in water. For special applications in water or other polar liquid environments, a surfactant with a modified polarized functional group should be adopted. In our study, 3-(N,N-Dimethylmyristylammonio)propanesulfonate (DP) is adopted as surfactants to fabricate modified magnetic nanoparticles which can be dispersed in the polar carrier liquid to further fabricate ferrofluids. The structural formulae of oleic acid and DP are shown in **Figure 1**. The oleic acid-covered nanoparticles are settled as a control group to identify the factors which are responsible for the colloidal stability in polar or apolar base liquid. Oleic acid-covered particles (P1) can be dispersed into apolar carrier liquid. In contrast, DP-coated magnetite nanopowders (P2) can only be separated into polar liquids such as water and ethanol (ε_r larger than 5). The use of surfactant DP is intended to permit the synthesis of a polar solvent-based colloidal suspension of magnetic nanoparticles. In order to justify the properties of the cover layers on particles, several theoretical models combined with experiment results are raised. This study is meaningful for us to understand the fitting relationships between surfactants and nanoparticles. It can become a guideline in choosing the right surfactants for a specific base fluid.

EXPERIMENTAL

Materials

Materials include ferric chloride hexahydrate powders ($FeCl_3{\cdot}6H_2O$, 99%), ferrous chloride tetrahydrate powders ($FeCl_2{\cdot}4H_2O$, 99%), ammonium hydroxide ($NH_3{\cdot}H_2O$, 25%), oleic acid (OA, $C_{18}H_{34}O_2$, 95%), 3-(N,N-dimethylmyristylammonio)propanesulfonate (DP, 98%), ethanol (p.a.), hexamethylene (p.a.), and carbon tetrachloride (p.a.). Most of these chemicals used for the synthesis of magnetic particles were purchased from Alfa Aesar and Macklin Biochemical Company. The probe agents adopted for contact angle measurement, that is, water (WT), formamide (FA), and ethanediol (ED), were purchased from Macklin Biochemical Company.

Nanoparticle Synthesis

The chemical co-precipitation approach was used to produce bare magnetic particles (Laurent et al., 2008; Rebodos and Vikesland, 2010; Cui et al., 2015; Rajput et al., 2016). To begin with, 23.64 g of ferric chloride hexahydrate powders ($FeCl_3{\cdot}6H_2O$) and 9.94 g of ferrous chloride tetrahydrate powders ($FeCl_2{\cdot}4H_2O$) were dissolved into 300 ml deionized water. In order to fit the final stoichiometric ratio of Fe^{3+}: Fe^{2+} = 2: 1, the molar ratio of Fe^{3+}: Fe^{2+} = 1.75: 1 was adopted in initial reactants to compensate for the oxidation of Fe^{2+}. After heating the solvent to 80°C, 80 ml ammonium aquation (25%) was added under high-speed stirring (350 rpm) to adjust pH value to be higher than 9.5. Subsequently, the mixture reacted for 45 min at 80°C to ensure that Fe^{3+} and Fe^{2+} were fully converted into Fe_3O_4. Then the magnetic nanoparticles were separated by a permanent magnet and washed with deionized water and ethanol several times until the pH value was 7. The obtained uncoated bare magnetic nanoparticle (BM) was used as the precursor to fabricate surfactant covered particles. The precursor BM was evenly divided into two parts. One part of the BM was added to

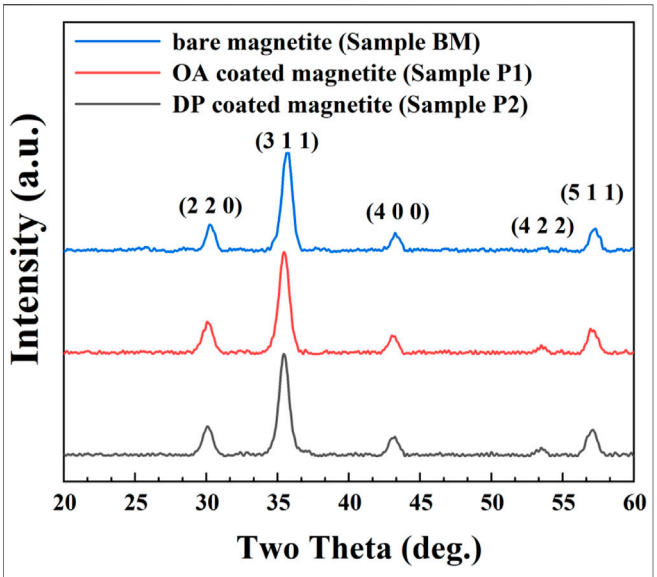

FIGURE 2 | XRD patterns of bare magnetite particles (BM), OA-coated particles (sample P1), and DP-coated magnetic nanoparticles (sample P2).

300 ml of deionized water. After the solvation process, 2 ml oleic acid was added to the solvation. In order to ensure that the particles were fully charged by H^+, pH was adjusted to six, lower than isoelectric point pH_{iep} = 6.5 (pH_{iep}: pH of zero zeta potential) (Galindo-González et al., 2005; López-López et al., 2005; Kosmulski, 2016). The mixture was heated to 80°C with vigorous stirring. The reacting process was kept for 30 min to get the BM completely covered by oleic acid. The oleic acid-covered magnetic particles (P1) were washed with deionized water to remove the unreacted oleic acid. The other part of BM was added to 300 ml of deionized water in a similar process. After that, 2.5 g of DP was dissolved into the mixture. The pH of the mixture was adjusted to 6. The reaction temperature was maintained at 80°C. After reacting for 30 min, the DP covered magnetic particles (P2) were washed by hexamethylene to ensure the coated surfaces not to be destroyed. Finally, two kinds of coated nanoparticles were dehydrated in a vacuum oven at 60°C for 4 h.

Methods

The crystalline structure of surfactants covered and uncovered nanoparticles was characterized by X-ray diffraction (Rigaku miniflex 600). Microstructures of nanoparticles were observed using transmission electron microscopy (TEM, JEM-100CXII). The functional groups of particles were examined by Fourier transform infrared spectroscopy (FT-IR, Thermo Scientific Nicolet iS 50). The zeta potential measurements were performed on the Malvern Zetasizer Nano ZS90. The magnetic properties of the magnetic nanoparticles were exanimated by a vibrating sample magnetometer (VSM, BKT-4500). The contact angle measurements were performed on a goniometer and its image-analysis software (HKCA-15). Smooth surfaces of magnetic nanoparticles were fabricated by depositing particles on a glass slide. Due to the dispersing ability differences of nanoparticles in polar of apolar carrier liquid, carbon tetrachloride and ethanol were used to disperse oleic acid covered particles (P1) and DP covered magnetite nanopowders (P2) respectively. A volume of 10 ml of these suspensions (10% volume fraction of particles) was enough to prepare a thick and smooth surface. The slides with colloidal suspension on them were dried under ambient conditions for 24 h. After that, the deposited surface on glass slides was placed in a vacuum oven heated to 60°C for 1 h.

RESULTS AND DISCUSSION

Physical Chemical Properties of Magnetic Particles

The X-ray diffraction patterns for particles from bare magnetite (BM), OA-coated magnetite (P1), and DP-coated magnetite (P2) are presented in **Figure 2**, respectively. As shown in **Figure 2**, the diffraction peaks could be ascribed to the inverse spinel phase. The positions of diffraction peaks were remained alike for different samples. The coating process of surfactant would not change the crystalline. However, magnetite (Fe_3O_4, JCPDS no. 19-0629) and maghemite (γ-Fe_2O_3, JCPDS no. 39-1346) patterns could be well adjusted to the experimental results (the analogous inverse cubic spinel structure may be responsible for their similarity in crystalline) (Rodríguez-Arco et al., 2011a; Gyergyek et al., 2011). According to the experimental conditions, starting materials and potassium dichromate titration, the nanoparticles could be deduced as magnetite nanoparticles.

From the X-ray diffraction results, the average particle size could be estimated by the Scherrer formula (Rodríguez-Arco et al., 2011a; Manikandan et al., 2015):

$$d_a = \frac{\delta\lambda}{\beta \cos\theta}, \quad (1)$$

where d_a is the average nanoparticle size, δ is the shape factor (0.9 for spherical magnetite nanograins), λ is the x-ray wavelength of Cu-K_α = 0.154 nm, θ is the Bragg diffraction angle of a certain diffraction peak, and β is full width at half maximum of the diffraction peak (FWHM). According to the calculation result, the average diameters for samples BM, P1, and P2 were obtained as 10.27 ± 0.10 nm, 10.58 ± 0.10 nm, and 10.09 ± 0.10 nm, respectively.

Transmission Electron Microscope (TEM) images of BM, P1, and P2 magnetic particles are shown in **Figure 3**. As presented in **Figure 3A**, spherical magnetite particles with a mean diameter of 9.97 ± 0.10 nm were well depicted. The mean diameter results in the TEM image well corresponded with the XRD results. The core-shell structures of surfactant-covered magnetite nanoparticles are well presented in **Figures 3B,C**. The thickness of cover layers of P1 and P2 were different. In sample P1, a coating layer with a thickness of ~2–3 nm was mainly formed by surfactant OA. According to the physical and chemical properties of oleic acid under ambient conditions, the coating layer of P1 was a layer of liquid organic phase mainly composed of oleic acid attached to the magnetite surface. In contrast, the surfactant shell formed by DP only had a thickness

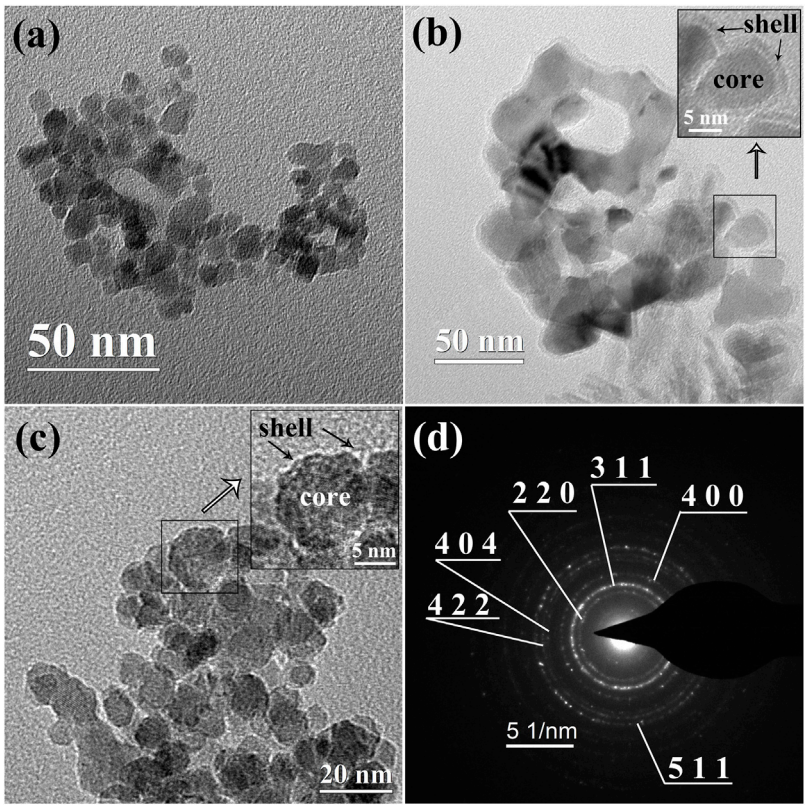

FIGURE 3 | TEM images of **(A)** BM magnetic nanoparticles, **(B)** P1 magnetic nanoparticles, and **(C)** magnetic nanoparticles P2. The inserts in **(B, C)** are the coating details in the selected area. **(D)**: selected area electron diffraction (SAED) of BM.

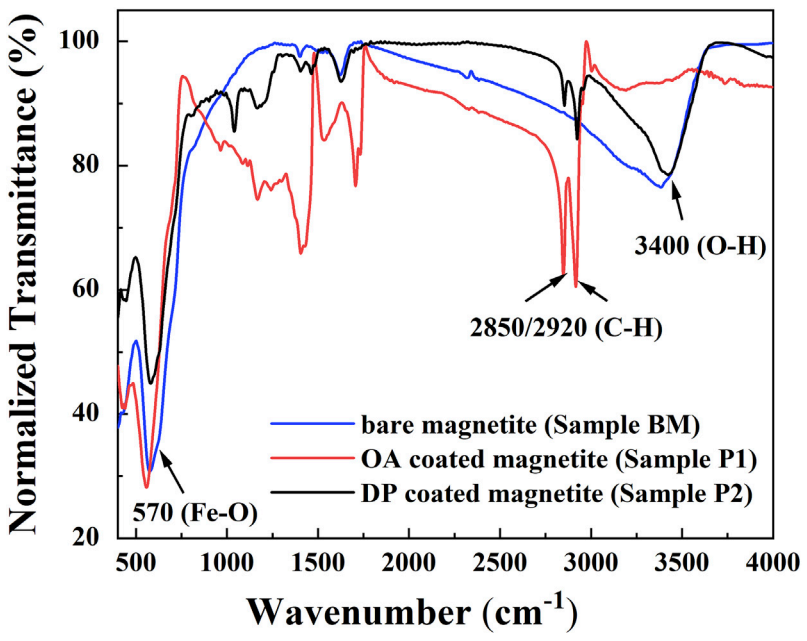

FIGURE 4 | FT-IR spectra of bare magnetite particles (BM), OA-coated particles (sample P1), and DP-coated magnetic nanoparticles (sample P2).

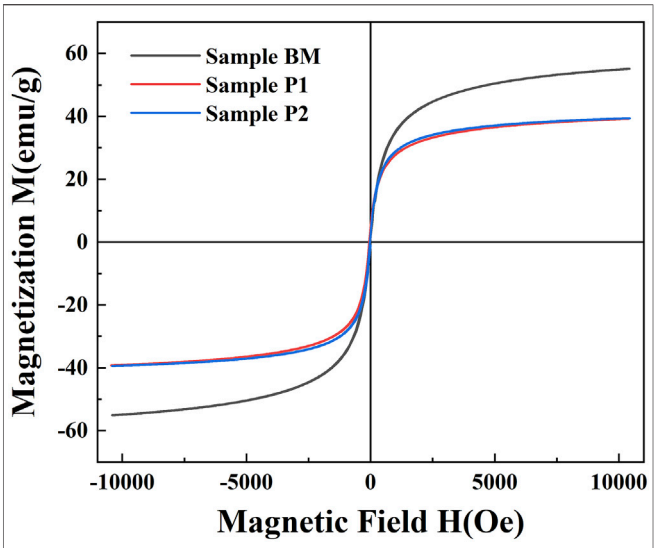

FIGURE 5 | Magnetization curves for bare magnetite particles (BM), OA-coated particles (sample P1), and DP-coated magnetic nanoparticles (sample P2).

of ~1 nm. Since the DP was solid under ambient conditions, the surfactant DP covering the magnetite was speculated to be the solid phase. The thin coating layer was unable to get the nanoparticles fully coated, which was attributed to the absence of surface tension in the solid-state coating layer. In **Figure 3D**, diffraction rings in electron diffraction are well fitted to the results of X-ray diffraction peaks, which is also an approvement of magnetite crystalline (Masui et al., 1997).

To further figure out the coating conditions of surfactant OA and DP, Fourier transform infrared measurements (FT-IR) were carried out. The FT-IR spectra results of BM, sample P1, and sample P2 are well depicted in **Figure 4**. As presented in **Figure 4**, sharp adsorption peaks at 570 cm^{-1} were obtained in all kinds of magnetic nanoparticles (Hong et al., 2006). The peaks at 570 cm^{-1} were attributed to the Fe-O bond. In samples P1 and P2, two sharp bonds at 2,850 cm^{-1} and 2,920 cm^{-1} were derived from the asymmetric CH_2 stretch and the symmetric CH_2 stretch, respectively (Zhang et al., 2006). This result was evidence of the presence of an organic coating layer on the magnetite particle surfaces. The strong peaks at 3,400 cm^{-1} were the demonstration of the exist of O-H on the particle surface (Cui et al., 2015). The functional group O-H on BM was the anchor point of surfactant. The disappearance of O-H in sample P1 was an indication that the functional group O-H was fully combined by OA. This result had the consistency of a thick coating layer of OA observed in the TEM image. The showing up of O-H in sample P2 was a piece of evidence that the particle surface was not fully coated by surfactant DP. This conclusion was also consistent with the TEM results.

The magnetization for bare magnetite particles (BM), OA-coated particles (sample P1), and DP-coated magnetic nanoparticles (sample P2) are shown in **Figure 5**. The hysteresis loops of nanoparticles had no remanence and coercivity. All the samples presented superparamagnetic properties. The saturated magnetization of BM, P1, and P2 were 55.1 emu/g, 39.3 emu/g, and 39.4 emu/g, respectively. The decreases in saturated magnetization in the coated magnetite samples were attributed to the non-magnetic surfactants.

In order to identify the colloidal stability of OA-coated particles and DP-coated particles in polar or apolar carrier liquid, water (polar, $\varepsilon_r > 5$) and carbon tetrachloride (apolar, $\varepsilon_r < 5$) were chosen as a base liquid to establish a colloidal system. As shown in **Figures 6B,C**, OA-coated particles could form a stable colloid system in an apolar carrier liquid. DP-coated nanoparticles underwent a severe phase separation in an apolar carrier liquid. As depicted in **Figures 6E,F**, DP-coated particles could form a stable colloidal system in polar carrier liquid while OA-coated particles could not. The particles coated by OA and DP had completely opposite stabilities in polar or apolar liquids. As shown in **Figures 6A,D**, uncoated magnetite particles could form a metastable colloidal system, which could be regarded as a standard to judge the stability of the colloidal system. Aiming to figure out the factors that contributed to the colloidal stability, theoretical analysis was performed in the colloidal systems of polar or apolar base liquid.

Theoretical Analysis of Colloidal Stability in Polar or Apolar Base Liquid

OA-coated magnetite nanoparticles (sample P1) could only be dispersed in the apolar organic base liquid ($\varepsilon_r < 5$) (López-López et al., 2005). In contrast, DP-coated magnetic particles (sample P2) could form stable colloidal solvation with a high particle concentration in the polar base fluid ($\varepsilon_r > 5$). The colloidal stability for magnetite particles dispersed in the apolar liquid could be explained by the Van Oss-Chaudhry-Good (VOCG) theory (Van Oss et al., 1988; van Oss, 1993) and surface free energy analysis. The total Gibbs free energy ΔG^{TOT} has multipart contributions of Lifshitz-van der Waals (LW) interaction, Lewis acid-base interaction, and steric repulsion potentials. The surface free energy could be obtained by measuring the surface tension (γ). Therefore, the surface tension of a material i can be expressed by Lifshitz-van der Waals part (γ_i^{LW}) and Lewis acid-base part (γ_i^{AB}) as:

$$\gamma_i = \gamma_i^{LW} + \gamma_i^{AB} = \gamma_i^{LW} + \sqrt{\gamma_i^+ \gamma_i^-}, \tag{2}$$

where γ_i^- and γ_i^+ are the electron-donor parameter and the electron-acceptor parameter. The Gibbs free energy of a certain solid surface (S) contacted by a certain liquid (L) could be calculated by the Young–Dupré equation and VOCG theory (van Oss, 1993):

$$\gamma_L (1 + \cos\theta) = 2\left(\sqrt{\gamma_S^{LW} \gamma_L^{LW}} + \sqrt{\gamma_S^+ \gamma_L^-} + \sqrt{\gamma_S^- \gamma_L^+} \right). \tag{3}$$

The surface tension components of a solid surface (γ_S^{LW}, γ_S^+ and γ_S^-) could be identified by three standard probe liquids. The probe liquids used in this study were water (WT), formamide (FA), and ethanediol (ED). The surface tension components of probe liquids are presented in **Table 1**.

In order to identify the solid surface free energy of oleic acid (OA) coated magnetic particles (sample P1) and 3-(N,N-Dimethylmyristylammonio)propanesulfonate (DP) coated

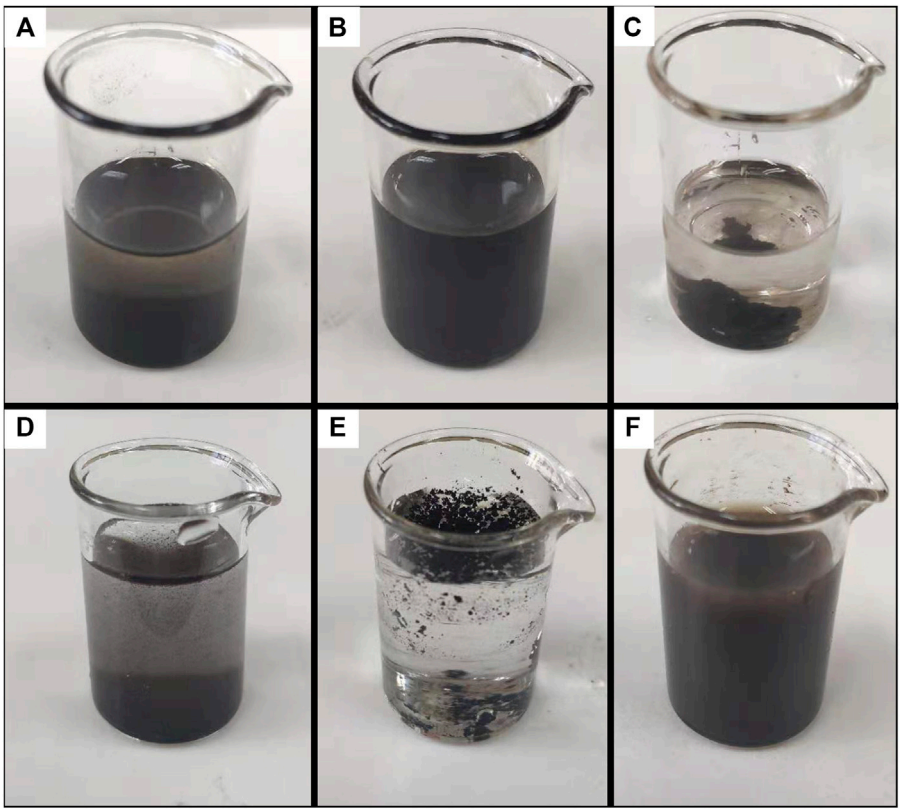

FIGURE 6 | Colloidal systems formed by magnetite particles coated by different surfactants in polar or apolar carrier liquid. **(A)** Uncoated particles in carbon tetrachloride. **(B)** OA-coated particles in carbon tetrachloride. **(C)** DP-coated particles in carbon tetrachloride. **(D)** Uncoated particles in water. **(E)** OA-coated particles in water. **(F)** DP-coated particles in water.

TABLE 1 | The electron-donor parameter γ_i^-, electron-acceptor parameter γ_i^+, Lifshitz-van der Waals part of surface tension (γ_i^{LW}), and total surface tension γ_L in probe liquids. All the units are in mJ/m^2. All the ambient temperatures of the surface tensions are at 20°C.

Liquid	γ_L	γ_i^{LW}	γ_i^+	γ_i^-
Water (WA)	72.8	21.8	25.5	25.5
Formamide (FA)	58.0	39.0	2.28	39.6
Ethanediol (ED)	48.0	29.0	1.92	47

The surface tension values of liquids are taken from Sawisai et al. (2019 and van Oss (1993).

TABLE 2 | The surface free energy components (mJ/m^2) of magnetite nanoparticles.

Samples	γ_i^{LW}	γ_i^+	γ_i^-
Bare magnetite[a]	49.3	0.17	55.4
OA-coated magnetite	24.4	0.00[c]	4.4
OA-coated magnetite[b]	25.3	0.15	5.2
DP-coated magnetite	92.3	0.00[c]	58.9

[a]*Taken from López-López et al. (2005) and Galindo-González et al. (2005).*
[b]*Taken from Shi et al. (2018) and López-López et al. (2005).*
[c]*The square root is negative. The error is larger than the value itself.*

nanoparticles (sample P2), the contact angle measurements were performed on smooth surfaces fabricated by magnetic particles. The results of contact angles measured on the surface of P1 were 95° ± 3° (water), 81° ± 5° (formamide), and 78° ± 5° (ethanediol). After that, contact angles are measured on the surface of P2 particles. The average results were 5° ± 1° (water), 8° ± 1° (formamide), and 15° ± 2° (ethanediol). The measured contact angles of OA-coated magnetite are consistent with the data in reference (López-López et al., 2005). Surface tension parameters could be obtained by solving **Eqs 2**, **3** using contact angles of probe liquids. The surface tension parameters are presented in **Table 2**. As shown in **Table 2**, the OA-coated magnetite surface shifted from a strong electron-donor property ($\gamma_i^+ \approx 0, \gamma_i^- = 55.4\, mJ/m^2$) on a bare magnetite surface to weak electron donor property ($\gamma_i^+ \approx 0$, $\gamma_i^- = 4.4\, mJ/m^2$). Meanwhile, the Lifshitz-van der Waals parameter was decreased on the OA-coated magnetite surface compared to the pure magnetite surface. The OA surfactant blocks the interaction between magnetite and carrier liquid. In contrast, DP-coated magnetite remained the same in electron-donor parameter and electron-acceptor parameter compared to the bare magnetite surface. The Lifshitz-van der Waals parameter (γ_i^{LW}), on DP covered magnetite surface was significantly increased from 49.3 mJ/m^2 to 92.3 mJ/m^2. The properties and working mechanisms of the

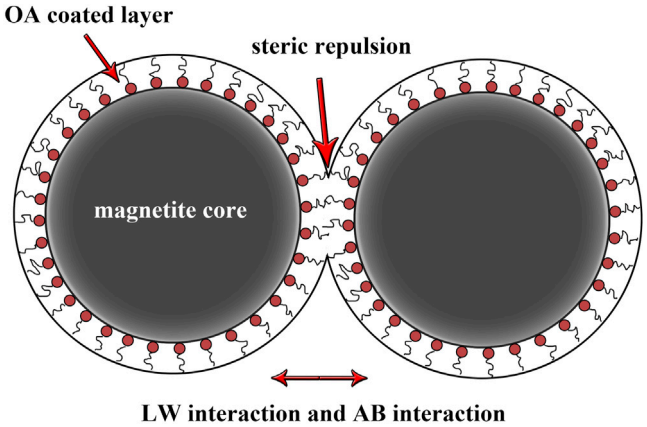

FIGURE 7 | Lifshitz-van der Waals (LW) interaction, acid-base (AB) interaction, and steric repulsion between OA-coated magnetite particles.

OA surfactant cover layer and DP surfactant cover layer were different.

In the apolar carrier liquid (phase 1), the colloidal stability of OA-coated magnetite particles (phase 2) could be explained by the surface free energy of Lifshitz-van der Waals (ΔG_{121}^{LW}), acid-base interaction (ΔG_{121}^{AB}), and steric repulsion (ΔG_{121}^{ST}). Steric interaction between particles in an apolar liquid phase is presented in **Figure 7**. Although DP-coated magnetite particles (phase 3) had a larger ΔG_{131}^{LW} due to their higher γ_i^{LW} compared to OA-coated particles, DP-coated particles almost had no steric repulsion between their solid phase thin cover layers. The steric repulsion ΔG_{121}^{ST} could be one of the main contributions to the colloidal stability in the apolar carrier liquid (Rodríguez-Arco et al., 2011b; Gyergyek et al., 2011). This may explain why OA-coated magnetic nanoparticles (P1 sample) could be dispersed in the polar organic liquid ($\varepsilon_r < 5$) to form a stable colloidal system, while DP-coated magnetite could not.

In the polar carrier liquid, the cohesion between carrier liquid molecular particles and hydrophilic magnetite particles was stronger due to their larger van der Waals force and hydrogen bond (van Oss, 2007). According to the DLVO theory, the colloidal nanoparticles could establish an electrical double layer (EDL). The potential of a shear plane in EDL is the zeta potential. As shown in **Figures 8A,B**, the zeta potential associated with electrical repulsion is one of the important contributions to the colloidal stability of ferrofluids. According to our experimental results, the zeta potentials of DP-coated magnetite under neutral conditions (pH = 7) in water and ethanol colloidal systems were 29.7 and 26.0 mV, respectively. According to the reference (Galindo-González et al., 2005), the zeta potential of uncoated magnetite particles was supposed to be −12 mV in the neutral water colloidal system. The DP surfactant coating layer on the magnetite surface was responsible for this zeta potential increase. This could be explained by the zeta potential presented in **Figure 8B**. As shown in **Figure 8B**, the surfactant DP, which could be seen as an electrical dipole, had its own electrical potential. The zeta potential (φ_{z2}) of DP-coated magnetite particles was calculated by adding the electrical

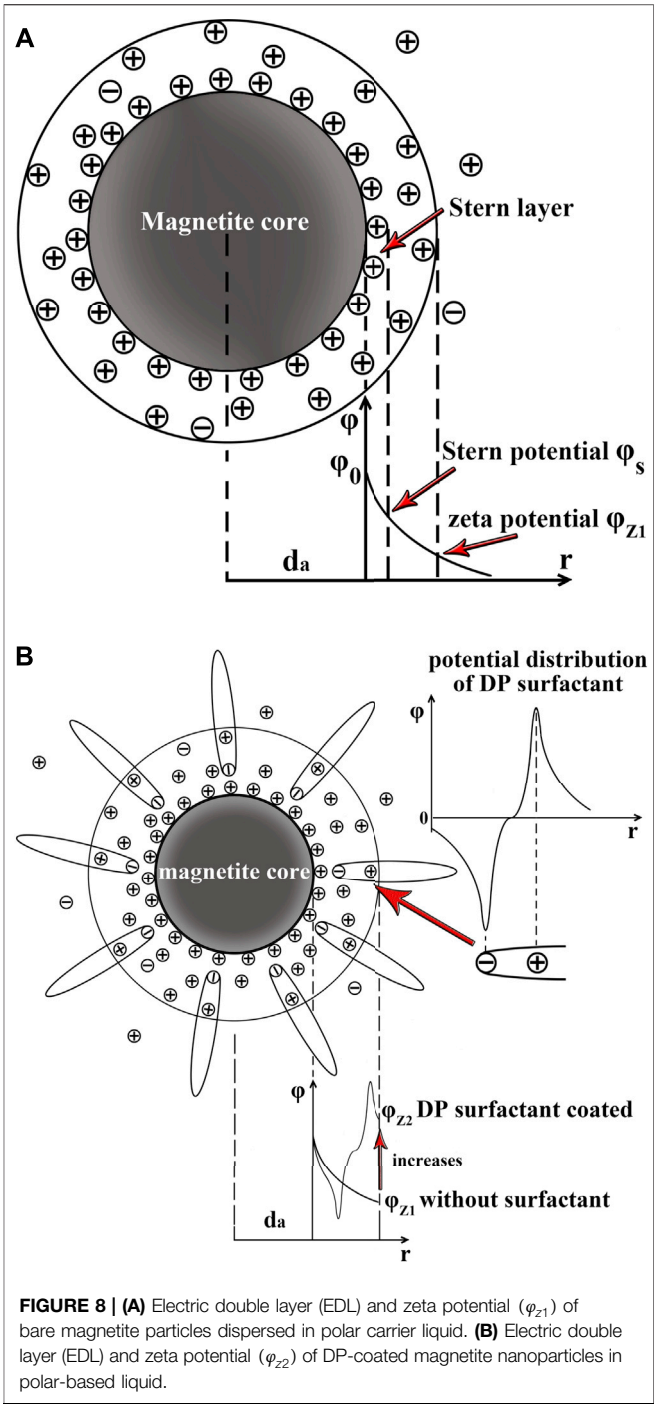

FIGURE 8 | (A) Electric double layer (EDL) and zeta potential (φ_{z1}) of bare magnetite particles dispersed in polar carrier liquid. **(B)** Electric double layer (EDL) and zeta potential (φ_{z2}) of DP-coated magnetite nanoparticles in polar-based liquid.

potential of the surfactant DP to the zeta potential φ_{z1} of bare magnetite particles.

Finally, the Lifshitz-van der Waals part (ΔG_{131}^{LW}), acid-base interaction part (ΔG_{131}^{AB}), and electrical repulsion part (ΔG_{131}^{EL}) of interfacial Gibbs free energy (1 = DP-coated magnetite, 3 = water) were calculated. ΔG_{131}^{LW} was obtained by **Eq. 4** (Gyergyek et al., 2011; Galindo-González et al., 2005; Gregory, 1981) and **(5)** (Gregory, 1981; Galindo-González et al., 2005; Gyergyek et al., 2011):

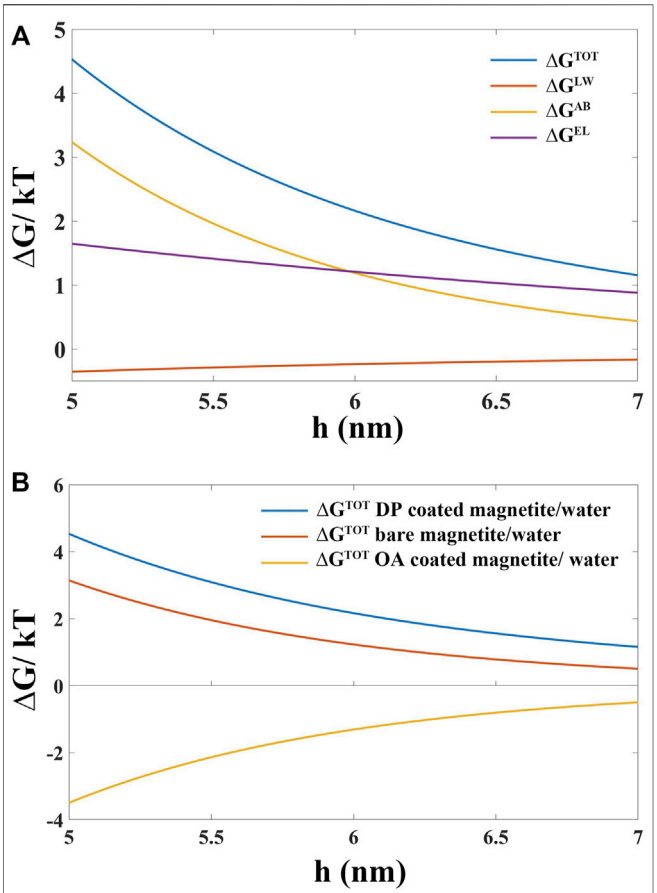

FIGURE 9 | (A) Interfacial distance (h) dependence of total surface interaction free energy (ΔG_{131}^{TOT}), Lifshitz-van der Waals part (ΔG_{131}^{LW}), acid-base interaction part (ΔG_{131}^{AB}) , and electrical part (ΔG_{131}^{EL}) of interfacial Gibbs free energy between magnetic particles coated by DP under water-based neutral condition (pH = 7). **(B)** Interfacial distance (h) dependence of total surface interaction free energy (ΔG_{sws}^{TOT}) of DP-coated magnetite, bare magnetite, and OA-coated magnetite in the neutral water-based colloidal system.

$$\Delta G_{131}^{LW}(h) = -\frac{A_{131}}{6}\left[\frac{2d_a^2}{h(4d_a+h)} - \frac{2d_a^2}{(2d_a+h)^2} + \ln\frac{h(4d_a+h)}{(2d_a+h)^2}\right], \tag{4}$$

$$A_{131} = 24\pi h_0^2\left(\sqrt{\gamma_1^{LW}} - \sqrt{\gamma_3^{LW}}\right)^2, \tag{5}$$

where d_a is the average diameter of nanoparticles. h_0 is the minimum equilibrium distance between interfaces, which is supposed to be $1.58 \pm 0.08\,\AA$ in a water-based colloidal system (Galindo-González et al., 2005; Gyergyek et al., 2011). h is the distance between neighbor interfaces of nanoparticles in the colloidal system. A_{131} is the Hamaker constant.

ΔG_{131}^{AB} was calculated by **Eq. 6** (van Oss, 1993; López-López et al., 2005; Gyergyek et al., 2011) and **(7)** (van Oss, 1993; Galindo-González et al., 2005):

$$\Delta G_{131}^{AB}(h_0) = -4\left(\sqrt{\gamma_1^+} - \sqrt{\gamma_3^+}\right)\left(\sqrt{\gamma_1^-} - \sqrt{\gamma_3^-}\right), \tag{6}$$

$$\Delta G_{131}^{AB}(h) = \Delta G_{131}^{AB}(h_0)\pi\lambda d_a\, exp\left(\frac{h_0 - h}{\lambda}\right), \tag{7}$$

where λ is the correlation length, or the decay length of the molecules of liquid medium (in water, $\lambda \approx 1\,nm$) (van Oss, 1993). d_a, h_0, and h have already been given in **Eqs 4**, **5**.

ΔG_{131}^{EL} was calculated by **Eq. 8** (Galindo-González et al., 2005) and **(9)** (Galindo-González et al., 2005; Ueno et al., 2008; Rodríguez-Arco et al., 2011a):

$$\Delta G_{131}^{EL}(h) = 2\pi\varepsilon_0\varepsilon_r d_a\zeta^2 \ln\left(1 + e^{-\kappa h}\right), \tag{8}$$

$$\kappa = \left(\frac{(2\times 10^3)N_A e^2 C_{eff}}{\varepsilon_0\varepsilon_r kT}\right)^{1/2}, \tag{9}$$

where ε_r is the dielectric constant of the carrier liquid, ε_0 is the permittivity of vacuum, ζ is the zeta potential of particles, d_a is the average diameter of magnetite particles, κ is the reciprocal Debye length. h is the average distance between neighbor interfaces of nanoparticles in the colloidal system, N_A is Avogadro's number, e is electronic charge, k (k_B) is Boltzmann constant, T is the absolute temperature (room temperature, 293.15 K), and C_{eff} is effective ionic charge concentration (the surfactant concentration is the main contribution to C_{eff}. Based on the amount of the surfactant, $C_{eff} \approx 0.01 mol\,L^{-1}$, the Debye length $\kappa^{-1} = 3\,nm$).

Total interaction surface free energy (ΔG_{131}^{TOT}) between DP-coated magnetic particles dispersed into water was the sum of the Lifshitz-van der Waals part (ΔG_{131}^{LW}), acid-base interaction part (ΔG_{131}^{AB}) , and electrical part (ΔG_{131}^{EL}) of interfacial Gibbs free energy:

$$\Delta G_{131}^{TOT}(h) = \Delta G_{131}^{LW}(h) + \Delta G_{131}^{AB}(h) + \Delta G_{131}^{EL}(h). \tag{10}$$

As shown in **Figure 9A**, the total interfacial free energy ΔG_{131}^{TOT} between magnetic particles coated by DP under neutral water-based conditions (a typical polar liquid-based colloidal system) is calculated. According to the Debye length ($\kappa^{-1} = 3\,nm$) result which was the thickness of EDL, the proper value of interfacial distance h between two particles was 6 nm (2 times of Debye length κ^{-1}). At this point, the main repulsion contributions of ΔG_{131}^{TOT} were electrical double layer repulsion energy ($\Delta G_{131}^{EL}(6nm) = 1.2\,k_BT$) and acid-base interaction surface interfacial energy ($\Delta G_{131}^{AB}(6nm) = 1.2\,k_BT$). The contribution of $\Delta G_{131}^{LW}(6\,nm)$ was - $0.2\,k_BT$, which indicated that the L-W force between magnetite particles was a mild attractive force. The total interfacial free energy ($\Delta G_{131}^{TOT}(6\,nm)$) of 2.2 k_BT (larger than the Brownian free energy of 1.5 k_BT) was large enough to resist the precipitation resulting from the gravitational field. If magnetite particles were not coated by DP, $\Delta G_{131}^{EL}(6\,nm)$ would significantly decrease from 1.2 k_BT to 0.1 k_BT (assuming the ionic concentration was maintained) due to the smaller zeta potential and ionic concentration. As shown in **Figure 9B**, the total interfacial free energy $\Delta G_{131}^{TOT}(6\,nm)$ of bare magnetite particles not coated by DP was reduced from 2.2 k_BT to 1.2 k_BT. The colloidal stability became fragile due to the absence of EDL repulsion. If the OA-coated magnetite particles were dispersed into water, ΔG_{121}^{TOT} would decrease to

-1.3 k_BT. This could be a plausible reason for a severe phase separation between OA-coated magnetite and water.

CONCLUSION

The coating state and colloidal stability of oleic acid (OA) and 3-(N,N-Dimethylmyristylammonio)propanesulfonate (DP) coated magnetite nanoparticles in the polar and apolar carrier liquid were systematically studied. Bare magnetite particles (with an average diameter of 10 nm), as precursors to fabricate surfactant-coated nanoparticles, were prepared by coprecipitation of Fe^{3+} and Fe^{2+} under aqueous conditions. The OA surfactant covering layer was a thick oil-state shell (~2–3 nm) which enabled the magnetite surface to be fully coated. The DP coating layer was a kind of solid-state thin shell (~1 nm), which did not allow the surface of magnetite to be fully coated. Different coating states enabled OA- and DP-coated magnetite particles to be dispersed in the base liquid with different dielectric constant ε_r. OA-coated magnetite particles could only be dispersed in the apolar carrier liquid ($\varepsilon_r < 5$) to form a stable colloidal system. In contrast, DP-coated magnetite particles could establish a stable dispersion in the polar base liquid ($\varepsilon_r > 5$). The stable colloidal system of OA covered magnetite in apolar base liquid was attributed to the steric repulsion of thick organic coating layers. Due to the solid-state thin coating layer, the DP-coated particles could not establish an organic barrier to keep adjacent nanoparticles from precipitation in the apolar carrier liquid system. From the calculating results of total Gibbs interfacial free energy ΔG_{131}^{TOT} in a neutral water-based colloidal system (a typical polar carrier liquid system), DP-coated magnetite particles had the highest $\Delta G_{131}^{TOT} = 2.2\,k_BT$. This high value of repulsive energy was the reason why DP-coated magnetite could form a stable dispersion in a water-based colloidal system. Bare magnetite particles could form a compared fragile colloidal system for its smaller $\Delta G_{131}^{TOT} = 1.2\,k_BT$ in neutral water base liquid. The shrinkage of interfacial free energy ΔG_{131}^{TOT} was attributed to the weak interparticle EDL electric repulsion (zeta potential reduced from 29.7 mV to -12 mV). The interparticle EDL electric repulsion was an important factor for the polar liquid-based colloidal system. The OA-coated particles had the lowest $\Delta G_{131}^{TOT} = -1.3\,k_BT$. The negative interfacial free energy indicated a strong attraction force between neighbor OA-coated nanoparticles in a water-based colloidal system. As a result, severe phase separation between OA-coated magnetite and water occurred.

DATA AVAILABILITY STATEMENT

The original contributions presented in the study are included in the article/Supplementary Material; further inquiries can be directed to the corresponding author.

AUTHOR CONTRIBUTIONS

LL: research, experiments, and manuscript. DL: teacher and adviser. ZZ: teacher and adviser.

FUNDING

This research is supported by the National Natural Science Foundation of China (No. 51735006, No. 51927810, and No. U1837206) and Beijing Municipal Natural Science Foundation (No. 3182013).

REFERENCES

Cui, H., Li, D., and Zhang, Z. (2015). Preparation and Characterization of Fe_3O_4 Magnetic Nanoparticles Modified by Perfluoropolyether Carboxylic Acid Surfactant. *Mater. Lett.* 143, 38–40. doi:10.1016/j.matlet.2014.12.037

Dailey, J. P., Phillips, J. P., Li, C., and Riffle, J. S. (1999). Synthesis of Silicone Magnetic Fluid for Use in Eye Surgery. *J. Magnetism Magnetic Mater.* 194, 140–148. doi:10.1016/s0304-8853(98)00562-9

Etemadi, H., and Plieger, P. G. (2020). Improvements in the Organic-Phase Hydrothermal Synthesis of Monodisperse MxFe3-xO4 (M = Fe, Mg, Zn) Spinel Nanoferrites for Magnetic Fluid Hyperthermia Application. *ACS omega* 5, 18091–18104. doi:10.1021/acsomega.0c01641

Galindo-González, C., de Vicente, J., Ramos-Tejada, M. M., López-López, M. T., González-Caballero, F., and Durán, J. D. G. (2005). Preparation and Sedimentation Behavior in Magnetic Fields of Magnetite-Covered Clay Particles. *Langmuir* 21, 4410–4419. doi:10.1021/la047393q

Gregory, J. (1981). Approximate expressions for retarded van der waals interaction. *J. Colloid Interface Sci.* 83, 138–145. doi:10.1016/0021-9797(81)90018-7

Gyergyek, S., Makovec, D., and Drofenik, M. (2011). Colloidal Stability of Oleic- and Ricinoleic-Acid-Coated Magnetic Nanoparticles in Organic Solvents. *J. Colloid Interface Sci.* 354, 498–505. doi:10.1016/j.jcis.2010.11.043

Hartshorne, H., Backhouse, C. J., and Lee, W. E. (2004). Ferrofluid-based Microchip Pump and Valve. *Sensors Actuators B Chem.* 99, 592–600. doi:10.1016/j.snb.2004.01.016

Hong, R. Y., Li, J. H., Li, H. Z., Ding, J., Zheng, Y., and Wei, D. G. (2008). Synthesis of Fe3O4 Nanoparticles without Inert Gas Protection Used as Precursors of Magnetic Fluids. *J. Magnetism Magnetic Mater.* 320, 1605–1614. doi:10.1016/j.jmmm.2008.01.015

Hong, R. Y., Pan, T. T., and Li, H. Z. (2006). Microwave Synthesis of Magnetic Fe_3O_4 Nanoparticles Used as a Precursor of Nanocomposites and Ferrofluids. *J. Magnetism Magnetic Mater.* 303, 60–68. doi:10.1016/j.jmmm.2005.10.230

Jain, N., Zhang, X., Hawkett, B. S., and Warr, G. G. (2011). Stable and Water-Tolerant Ionic Liquid Ferrofluids. *ACS Appl. Mat. Interfaces* 3, 662–667. doi:10.1021/am1012112

Kosmulski, M. (2016). Isoelectric Points and Points of Zero Charge of Metal (Hydr) oxides: 50years after Parks' Review. *Adv. colloid interface Sci.* 238, 1–61. doi:10.1016/j.cis.2016.10.005

Kumar, P., Khanduri, H., Pathak, S., Singh, A., Basheed, G. A., and Pant, R. P. (2020). Temperature Selectivity for Single Phase Hydrothermal Synthesis of PEG-400 Coated Magnetite Nanoparticles. *Dalton Trans.* 49, 8672–8683. doi:10.1039/d0dt01318h

Kumar, P., Pathak, S., Jain, K., Singh, A., KuldeepBasheed, G. A., et al. (2022). Low-temperature Large-Scale Hydrothermal Synthesis of Optically Active PEG-200 Capped Single Domain $MnFe_2O_4$ Nanoparticles. *J. Alloys Compd.* 904, 12. doi:10.1016/j.jallcom.2022.163992

Kumar, P., Pathak, S., Singh, A., Khanduri, H., KuldeepJain, K., et al. (2021). Enhanced Static and Dynamic Magnetic Properties of PEG-40 0 Coated $CoFe_2$-xErxO4 (0.7 X 0) Nanoferrites. *J. Alloys Compd.* 887, 24. doi:10.1016/j.jallcom.2021.161418

Laurent, S., Forge, D., Port, M., Roch, A., Robic, C., Vander Elst, L., et al. (2008). Magnetic Iron Oxide Nanoparticles: Synthesis, Stabilization, Vectorization, Physicochemical Characterizations, and Biological Applications. *Chem. Rev.* 108, 2064–2110. doi:10.1021/cr068445e

Lobaz, V., Klupp Taylor, R. N., and Peukert, W. (2012). Highly Magnetizable Superparamagnetic Colloidal Aggregates with Narrowed Size Distribution from Ferrofluid Emulsion. *J. Colloid Interface Sci.* 374, 102–110. doi:10.1016/j.jcis.2012.01.057

López-López, M. T., Durán, J. D. G., Delgado, A. V., and González-Caballero, F. (2005). Stability and Magnetic Characterization of Oleate-Covered Magnetite Ferrofluids in Different Nonpolar Carriers. *J. Colloid Interface Sci.* 291, 144–151. doi:10.1016/j.jcis.2005.04.099

Manikandan, A., Saravanan, A., Antony, S. A., and Bououdina, M. (2015). One-Pot Low Temperature Synthesis and Characterization Studies of Nanocrystalline α-Fe_2O_3 Based Dye Sensitized Solar Cells. *J. Nanosci. Nanotechnol.* 15, 4358–4366. doi:10.1166/jnn.2015.9804

Masui, T., Fujiwara, K., Machida, K.-i., Adachi, G.-y., Sakata, T., and Mori, H. (1997). Characterization of Cerium(IV) Oxide Ultrafine Particles Prepared Using Reversed Micelles. *Chem. Mat.* 9, 2197–2204. doi:10.1021/cm970359v

Medeiros, A. M. M. S., Parize, A. L., Oliveira, V. M., Neto, B. A. D., Bakuzis, A. F., Sousa, M. H., et al. (2012). Magnetic Ionic Liquids Produced by the Dispersion of Magnetic Nanoparticles in 1-N-Butyl-3-Methylimidazolium Bis(trifluoromethanesulfonyl)imide (BMI.NTf2). *ACS Appl. Mat. Interfaces* 4, 5458–5465. doi:10.1021/am301367d

Okabe, T., Moritaka, D., Miyatake, M., Kondo, Y., Sasaki, S., and Yoshimoto, S. (2017). Development and Performance of a Magnetic Ionic Liquid for Use in Vacuum-Compatible Non-contact Seals. *Precis. Eng.* 47, 97–103. doi:10.1016/j.precisioneng.2016.07.010

Pathak, S., Jain, K., Kumar, P., Wang, X., and Pant, R. P. (2019). Improved Thermal Performance of Annular Fin-Shell Tube Storage System Using Magnetic Fluid. *Appl. Energy* 239, 1524–1535. doi:10.1016/j.apenergy.2019.01.098

Rajput, S., Pittman, C. U., and Mohan, D. (2016). Magnetic Magnetite (Fe_3O_4) Nanoparticle Synthesis and Applications for Lead (Pb^{2+}) and Chromium (Cr^{6+}) Removal from Water. *J. Colloid Interface Sci.* 468, 334–346. doi:10.1016/j.jcis.2015.12.008

Rebodos, R. L., and Vikesland, P. J. (2010). Effects of Oxidation on the Magnetization of Nanoparticulate Magnetite. *Langmuir* 26, 16745–16753. doi:10.1021/la102461z

Rodríguez-Arco, L., López-López, M. T., Durán, J. D., Zubarev, A., and Chirikov, D. (2011). Stability and Magnetorheological Behaviour of Magnetic Fluids Based on Ionic Liquids. *J. Phys. Condens Matter* 23, 455101. doi:10.1088/0953-8984/23/45/455101

Rodríguez-Arco, L., López-López, M. T., González-Caballero, F., and Durán, J. D. G. (2011). Steric Repulsion as a Way to Achieve the Required Stability for the Preparation of Ionic Liquid-Based Ferrofluids. *J. Colloid Interface Sci.* 357, 252–254. doi:10.1016/j.jcis.2011.01.083

Saputro, R. E., Taufiq, A., SunaryonoHidayat, N., and Hidayat, A. (2020). Effects of DMSO Content on the Optical Properties, Liquid Stability, and Antimicrobial Activity of Fe3O4/OA/DMSO Ferrofluids. *Nano* 15, 10. doi:10.1142/s1793292020500678

Sawisai, R., Wanchanthuek, R., Radchatawedchakoon, W., and Sakee, U. (2019). Simple Continuous Flow Synthesis of Linoleic and Palmitic Acid-Coated Magnetite Nanoparticles. *Surfaces Interfaces* 17, 11. doi:10.1016/j.surfin.2019.100344

Shi, X., Huang, W., and Wang, X. (2018). Ionic Liquids-Based Magnetic Nanofluids as Lubricants. *Lubr. Sci.* 30, 73–82. doi:10.1002/ls.1405

Torres-Díaz, I., and Rinaldi, C. (2014). Recent Progress in Ferrofluids Research: Novel Applications of Magnetically Controllable and Tunable Fluids. *Soft Matter* 10, 8584–8602. doi:10.1039/c4sm01308e

Ueno, K., Inaba, A., Kondoh, M., and Watanabe, M. (2008). Colloidal Stability of Bare and Polymer-Grafted Silica Nanoparticles in Ionic Liquids. *Langmuir* 24, 5253–5259. doi:10.1021/la704066v

van Oss, C. J. (1993). Acid-base Interfacial Interactions in Aqueous Media. *Colloids Surfaces A Physicochem. Eng. Aspects* 78, 1–49. doi:10.1016/0927-7757(93)80308-2

van Oss, C. J. (2007). Development and Applications of the Interfacial Tension between Water and Organic or Biological Surfaces. *Colloids Surfaces B Biointerfaces* 54, 2–9. doi:10.1016/j.colsurfb.2006.05.024

Van Oss, C. J., Good, R. J., and Chaudhury, M. K. (1988). Additive and Nonadditive Surface Tension Components and the Interpretation of Contact Angles. *Langmuir* 4, 884–891. doi:10.1021/la00082a018

Zhang, L., He, R., and Gu, H.-C. (2006). Oleic Acid Coating on the Monodisperse Magnetite Nanoparticles. *Appl. Surf. Sci.* 253, 2611–2617. doi:10.1016/j.apsusc.2006.05.023

Conflict of Interest: The authors declare that the research was conducted in the absence of any commercial or financial relationships that could be construed as a potential conflict of interest.

Publisher's Note: All claims expressed in this article are solely those of the authors and do not necessarily represent those of their affiliated organizations, or those of the publisher, the editors, and the reviewers. Any product that may be evaluated in this article, or claim that may be made by its manufacturer, is not guaranteed or endorsed by the publisher.